Ballbar based geometric error measurement and uncertainty analysis of rotary axis for five-axis machine

Jianghao Sun, Sitong Xiang*, Ben Yu, Maolei Chen
Faculty of Mechanical Engineering and Mechanics, Ningbo University, Ningbo 315211, China

ABSTRACT

The ballbar is currently the most widely used instrument for identifying and measuring rotary axis geometric errors, but the measurement results are unreliable due to measurement defects. So the geometric error measurement and uncertainty evaluation method based on ballbar is proposed. Firstly, the radial, tangential and axial measurement are carried out with the ballbar, and the geometric errors are identified according to the eccentricity and deviation of the trajectory. Then, by clarifying the mechanism of uncertainty caused by the tool setting error, ballbar installation error and translational axis error, the evaluation model is established. Finally, this study uses the Monte Carlo method to analyze the measurement uncertainty. The results show that the tool setting error and translational axis error are the main sources of measurement uncertainty, and the measurement uncertainty of the angular positioning error is the largest, which is contributed by the sine and cosine terms in the error identification equation.

Keywords: Ballbar, geometric error measurement, uncertainty analysis

1. INTRODUCTION

Geometric error measurement and uncertainty analysis of rotary axis of five-axis machine is a difficult research point in recent years. The rotary axis geometric error directly affects the machining quality of the five-axis machine[1]. According to the causes and manifestations of the errors, the geometric errors of the rotary axis are mainly divided into: position-dependent geometric errors (PDGEs) and position-independent geometric errors (PIGEs)[2]. PDGEs can be understood as the non-ideal motion of the axis, which varies with rotation and is represented by a position-dependent function.

There are many PDGEs' measurement methods. He used a laser interferometer to measure by a dual optical path measurement method. The identification process only relies on simple algebraic relationships without volume error modeling, which is easier to understand[3]. Wang used laser tracker to identify rotation axis errors based on the idea of spatial sequence multiple points[4]. Deng considered rigid body motion constraints and used tracking interferometer measurements to effectively separate the rotational axis PDGE from the PIGE[5]. A ballbar is a commonly used instrument for measuring geometric errors, which can identify error terms from measurement data based on a kinematic model. However, since the measurement results are not necessarily reliable, uncertainty analysis is required[6].

Current uncertainty evaluation methods can be divided into GUM[7] and Monte Carlo method (MCM)[8]. MCM allows the evaluation of uncertainty without calculating the partial derivatives of the measurement model[9], which exactly matches the characteristics of ballbar's multiple input and output, so this study uses MCM to analyze the measurement uncertainty of the ballbar. Scholars often ignore tool setting error and translation axis motion error, and these two cannot be eliminated by compensation[10]. Therefore, both types of errors need to be considered when analyzing the measurement uncertainty of a ballbar.

In view of the above situation, this study established a geometric error model and carried out measurement uncertainty analysis based on MCM. The results of the uncertainty evaluation show the feasibility of this approach.

2. GEOMETRIC ERROR MEASUREMENT OF ROTARY AXIS

2.1 Kinematic model of five-axis machine

The structure of the five-axis machine used in this study is shown in Figure 1. The machine has a coordinate systems with five axes: X(XCS), Y(YCS), Z(ZCS), A(ACS) and C(CCS). In addition, there are bed (MCS), spindle (SCS),

* xiangsitong@nbu.edu.cn

Third International Conference on Computer Science and Communication Technology (ICCSCT 2022)
edited by Yingfa Lu, Changbo Cheng, Proc. of SPIE Vol. 12506, 125065U
 · 0277-786X · doi: 10.1117/12.2661756

cutting tool (TCS) and workpiece coordinate systems (WCS). According to the machine tool structure, the tool chain is MCS → YCS → XCS → ZCS → SCS → TCS and the workpiece chain is MCS → ACS → CCS → WCS.

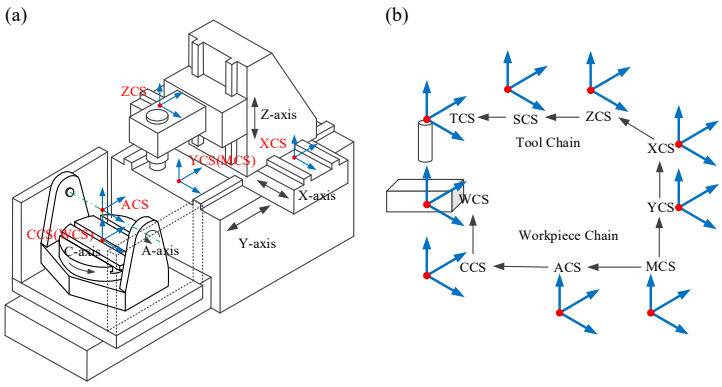

Figure 1. Five-axis machine structure and motion chain.

The distance between measuring ball's actual position P_{actual} and theoretical position P_{ideal} needs to be calculated. The the ball's position P_{actual_A} on the table side can be calculated by Equation (1). Where, E_A represents PDGEs error matrix, $T_{A\text{-}ideal}$ represents the ideal motion matrix, and P_0 represents the measurement ball's initial position. And the following study only takes the A-axis as an example for analysis.

$$\mathbf{P}_{\text{actual\_A}} = \mathbf{E}_{\text{A}} \cdot \mathbf{T}_{\text{A-ideal}} \cdot \mathbf{P}_0 \tag{1}$$

The length change of the ballbar $\Delta\mathbf{L}$ is based on the kinematic model, which is obtained by measuring the A-axis, as shown in Equation (2). Where, H represents the distance between the ball on the table side and the center line of the A-axis.

$$\Delta\mathbf{L}_{\text{A}} = \mathbf{P}_{\text{actual\_A}} - \mathbf{P}_{\text{ideal\_A}} = \begin{bmatrix} H\cdot\left(\sin(a)\cdot\varepsilon_{za}+\cos(a)\cdot\varepsilon_{ya}\right)+\delta_{xa} \\ L\cdot\varepsilon_{za}-H\cdot\cos(a)\cdot\varepsilon_{xa}+\delta_{ya} \\ -\varepsilon_{ya}\cdot L-H\cdot\sin(a)\cdot\varepsilon_{xa}+\delta_{za} \\ 0 \end{bmatrix} \tag{2}$$

2.2 Modeling and measurement of PDGEs

The error decomposition of the A-axis is performed in the measurement modes of three directions, and then the corresponding ballbar length variations Δl_{radial}, Δl_{tan}, and Δl_{axial} are obtained[11].

According to the error decomposition formula in Equation (2), the identification of A-axis PDGEs can be calculated by Equation (3).

$$\begin{cases} H\cdot\left(\sin(a)\cdot\varepsilon_{za}+\cos(a)\cdot\varepsilon_{ya}\right)+\delta_{xa} = -\Delta l_{\text{axial}} \\ \left(L\cdot\varepsilon_{za}-H\cdot\cos(a)\cdot\varepsilon_{xa}+\delta_{ya}\right)\cos(a)-\left(-\varepsilon_{ya}\cdot L-H\cdot\sin(a)\cdot\varepsilon_{xa}+\delta_{za}\right)\sin(a) = -\Delta l_{\text{tan}} \\ \left(L\cdot\varepsilon_{za}-H\cdot\cos(a)\cdot\varepsilon_{xa}+\delta_{ya}\right)\sin(a)+\left(-\varepsilon_{ya}\cdot L-H\cdot\sin(a)\cdot\varepsilon_{xa}+\delta_{za}\right)\cos(a) = -\Delta l_{\text{radial}} \end{cases} \tag{3}$$

During the measurement of A-axis PDGEs, the A-axis motion range is set from 0° to -90°, and the A-axis angle an is recorded every 15°. As shown in Equation (4), three measurement modes are performed under three different installation parameters, and Equation (3) is simplified to obtain the identification equations of PDGEs under different installation parameters. Where, L_{m} and H_{m} are different installation parameters at m-th test (m=1, 2, 3), and the subscript n of PDGEs corresponds to the A-axis motion angle a_n. $(\Delta l_{radial})_{m,n}$, $(\Delta l_{tan})_{m,n}$, and $(\Delta l_{axial})_{m,n}$ represent the variation of ballbar length corresponding to the A-axis motion angle a_n for radial, tangential, and axial measurements under m-th installation

parameters, respectively. By decoupling Equation (4), all PDGEs of the A-axis can be obtained, as shown in Equation (5). It is noticed here that there are two solutions for ε_{xa} in Equation 5(a). Different sine and cosine in the denominator will have different results, and the appropriate formula should be selected according to the angle.

$$\begin{cases} H_m \cdot \left(\sin(a_n)\cdot \varepsilon_{za,n} + \cos(a_n)\cdot \varepsilon_{ya,n}\right) + \delta_{xa,n} = -\left(\Delta l_{\text{axial}}\right)_{m,n} \\ L_m \cdot \varepsilon_{za,n} - H_m \cdot \cos(a_n)\cdot \varepsilon_{xa,n} + \delta_{ya,n} = -\left(\Delta l_{\tan}\right)_{m,n}\cdot\cos(a_n) - \left(\Delta l_{\text{radial}}\right)_{m,n}\cdot\sin(a_n) \\ -L_m \cdot \varepsilon_{ya,n} - H_m \cdot \sin(a_n)\cdot \varepsilon_{xa,n} + \delta_{za,n} = \left(\Delta l_{\tan}\right)_{m,n}\cdot\sin(a_n) - \left(\Delta l_{\text{radial}}\right)_{m,n}\cdot\cos(a_n) \end{cases} \tag{4}$$

$$\begin{cases} \left.\begin{aligned} \varepsilon_{xa,n} &= \frac{(Y_{1,n}-Y_{2,n})(L_1-L_3)-(Y_{1,n}-Y_{3,n})(L_1-L_2)}{\left[(L_1-L_2)(H_3-H_1)-(L_1-L_3)(H_2-H_1)\right]\cdot\cos(a_n)} \\ \varepsilon_{xa,n} &= \frac{(Z_{1,n}-Z_{2,n})(L_3-L_1)-(Z_{1,n}-Z_{3,n})(L_2-L_1)}{\left[(L_1-L_2)(H_3-H_1)-(L_1-L_3)(H_2-H_1)\right]\cdot\sin(a_n)} \end{aligned}\right\} & 5(a) \\ \varepsilon_{ya,n} = \frac{(Y_{1,n}-Y_{2,n})(H_3-H_1)-(Y_{1,n}-Y_{3,n})(H_2-H_1)}{(L_1-L_3)(H_1-H_2)-(L_1-L_2)(H_1-H_3)} & 5(b) \\ \varepsilon_{za,n} = \frac{(Z_{1,n}-Z_{2,n})(H_3-H_1)-(Z_{1,n}-Z_{3,n})(H_2-H_1)}{(L_1-L_3)(H_2-H_1)-(L_1-L_2)(H_3-H_1)} & 5(c) \\ \delta_{xa,n} = \frac{H_1\cdot X_{3,n} - H_3\cdot X_{1,n}}{H_1-H_3} & 5(d) \\ \delta_{ya,n} = Y_{2,n} + H_2\cdot\frac{(Y_{1,n}-Y_{2,n})(L_1-L_3)-(Y_{1,n}-Y_{3,n})(L_1-L_2)}{(L_1-L_2)(H_3-H_1)-(L_1-L_3)(H_2-H_1)} - L_2\cdot\frac{(Y_{1,n}-Y_{2,n})(H_3-H_1)-(Y_{1,n}-Y_{3,n})(H_2-H_1)}{(L_1-L_3)(H_1-H_2)-(L_1-L_2)(H_1-H_3)} & 5(e) \\ \delta_{za,n} = Z_{2,n} + H_2\cdot\frac{(Z_{1,n}-Z_{2,n})(L_3-L_1)-(Z_{1,n}-Z_{3,n})(L_2-L_1)}{(L_1-L_2)(H_3-H_1)-(L_1-L_3)(H_2-H_1)} + L_2\cdot\frac{(Z_{1,n}-Z_{2,n})(H_3-H_1)-(Z_{1,n}-Z_{3,n})(H_2-H_1)}{(L_1-L_3)(H_2-H_1)-(L_1-L_2)(H_3-H_1)} & 5(f) \end{cases} \tag{5}$$

3. MEASUREMENT UNCERTAINTY ANALYSIS

The influence of tool setting error, ballbar installation error and translational axis motion error on measurement uncertainty is considered. On this basis, an identification model $Y=f(X_1, X_2, \ldots, X_n)$ considering multiple error sources is established. Here the output Y is the PDGEs identification result and the input X_n is the source of uncertainty.

For the A-axis, the measurement model of the PDGEs can be expressed by Equation (6) after substituting the uncertainties introduced by the tool setting error, ballbar installation error, and translational axis motion error into Equation (3). Where, $(\Delta\rho_{\text{radial}})_{m,n}$, $(\Delta\rho_{\tan})_{m,n}$, $(\Delta\rho_{\text{axial}})_{m,n}$, $(\Delta x_{\text{t\_axis}})_{m,n}$, $(\Delta y_{\text{t\_axis}})_{m,n}$ and $(\Delta z_{\text{t\_axis}})_{m,n}$ are calculated by Equation (7). $\Delta x_{\text{t\_axis}}$, $\Delta y_{\text{t\_axis}}$, and $\Delta z_{\text{t\_axis}}$ are the errors in three directions caused by the translational axes motion error, respectively; Δh is the error caused by the tool setting error; $\Delta\rho_{\text{radial}}$, $\Delta\rho_{\tan}$, and $\Delta\rho_{\text{axial}}$ are the ballbar length variations in radial, tangential, and axial measurements caused by the installation error.

$$\begin{cases} H_m \cdot \left(\sin(a_n)\cdot \varepsilon_{za,n} + \cos(a_n)\cdot \varepsilon_{ya,n}\right) + \delta_{xa,n} = -\left(\Delta\rho_{\text{axial}}\right)_{m,n} + \left(\Delta x_{\text{t\_axis}}\right)_{m,n} \\ L_m \cdot \varepsilon_{za,n} - H_m \cdot \cos(a_n)\cdot \varepsilon_{xa,n} + \delta_{ya,n} = -\left(\Delta\rho_{\tan}\right)_{m,n}\cdot\cos(a_n) - \left(\Delta\rho_{\text{radial}}\right)_{m,n}\cdot\sin(a_n) + \left(\Delta y_{\text{t\_axis}}\right)_{m,n} \\ -L_m \cdot \varepsilon_{ya,n} - H_m \cdot \sin(a_n)\cdot \varepsilon_{xa,n} + \delta_{za,n} = \left(\Delta\rho_{\tan}\right)_{m,n}\cdot\sin(a_n) - \left(\Delta\rho_{\text{radial}}\right)_{m,n}\cdot\cos(a_n) + \left(\Delta z_{\text{t\_axis}}\right)_{m,n} + \Delta h \end{cases} \tag{6}$$

$$
\begin{cases}
(\Delta\rho_{\text{radial}})_{m,n} = \sqrt{\delta_{m,n}^2 + e_m^{\,2}} - \sqrt{\delta_{m,0}^2 + e_m^{\,2}} \\
(\Delta\rho_{\tan})_{m,n} = \sqrt{e_m^{\,2} + \delta_{m,n}^2 - 2e_m\delta_{m,n}\cos(\alpha_m + 90°)} - \sqrt{e_m^{\,2} + \delta_{m,0}^2 - 2e_m\delta_{m,0}\cos(\alpha_m + 90°)} \\
(\Delta\rho_{\text{axial}})_{m,n} = \sqrt{e_m^{\,2} + \delta_{m,n}^2 - 2e_m\delta_{m,n}\cos(\alpha_m)} - \sqrt{e_m^{\,2} + \delta_{m,0}^2 - 2e_m\delta_{m,0}\cos(\alpha_m)} \\
(\Delta x_{\text{t\_axis}})_{m,n} = \delta_{xx,n} + \delta_{xy,n} + \delta_{xz,n} + z_m\varepsilon_{yx,n} + z_m\varepsilon_{yy,n} + z_m S_{xz} \\
(\Delta y_{\text{t\_axis}})_{m,n} = \delta_{yx,n} + \delta_{yy,n} + \delta_{yz,n} + x_m\varepsilon_{zy,n} - z_m\varepsilon_{xx,n} - z_m\varepsilon_{xy,n} + x_m S_{xy} - z_m S_{yz} \\
(\Delta z_{\text{t\_axis}})_{m,n} = \delta_{zx,n} + \delta_{zy,n} + \delta_{zz,n} - x_m\varepsilon_{yy,n}
\end{cases} \tag{7}
$$

4. EXPERIMENTAL VERIFICATION

4.1 PDGEs identification and uncertainty evaluation

The PDGEs measurement experiments of the rotary axis are carried out on an AC rotary table five-axis machine. The measurement process is shown in Figure 2.

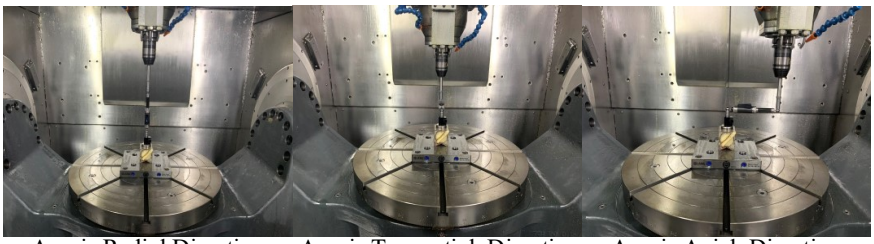

A-axis Radial Direction A-axis Tangential Direction A-axis Axial Direction

Figure 2. Ballbar measurements for A-axis.

In this study, the experiments of various geometric errors when a_n is 60° and the geometric errors ε_{xa} at different motion angles of the A-axis are carried out. The identification result is shown in Figure 3.

According to the uncertainty evaluation model of PDGEs, the tool setting error, ballbar installation error and translational axis motion error are sampled in the distribution interval with a sample size of M times in Monte Carlo test. For the inclusion probability $p = 0.95$, M is chosen to be 10^6 times in this study.

Substituting the above uncertainty sources into the uncertainty evaluation model, the M times output results of six PDGEs with different motion angles are obtained, which constitute the distribution of PDGEs output. The PDGEs output is sorted by non-decreasing order to obtain the identification results of PDGEs of A-axis under the influence of uncertainty sources, as shown in Figure 4. The results show that the uncertainty of the certain errors is very large compared to the geometric error itself. Due to the uncertainties vary at different angles, the mean values of the uncertainties of each geometric error of A-axis at different angles are shown in Table 1.

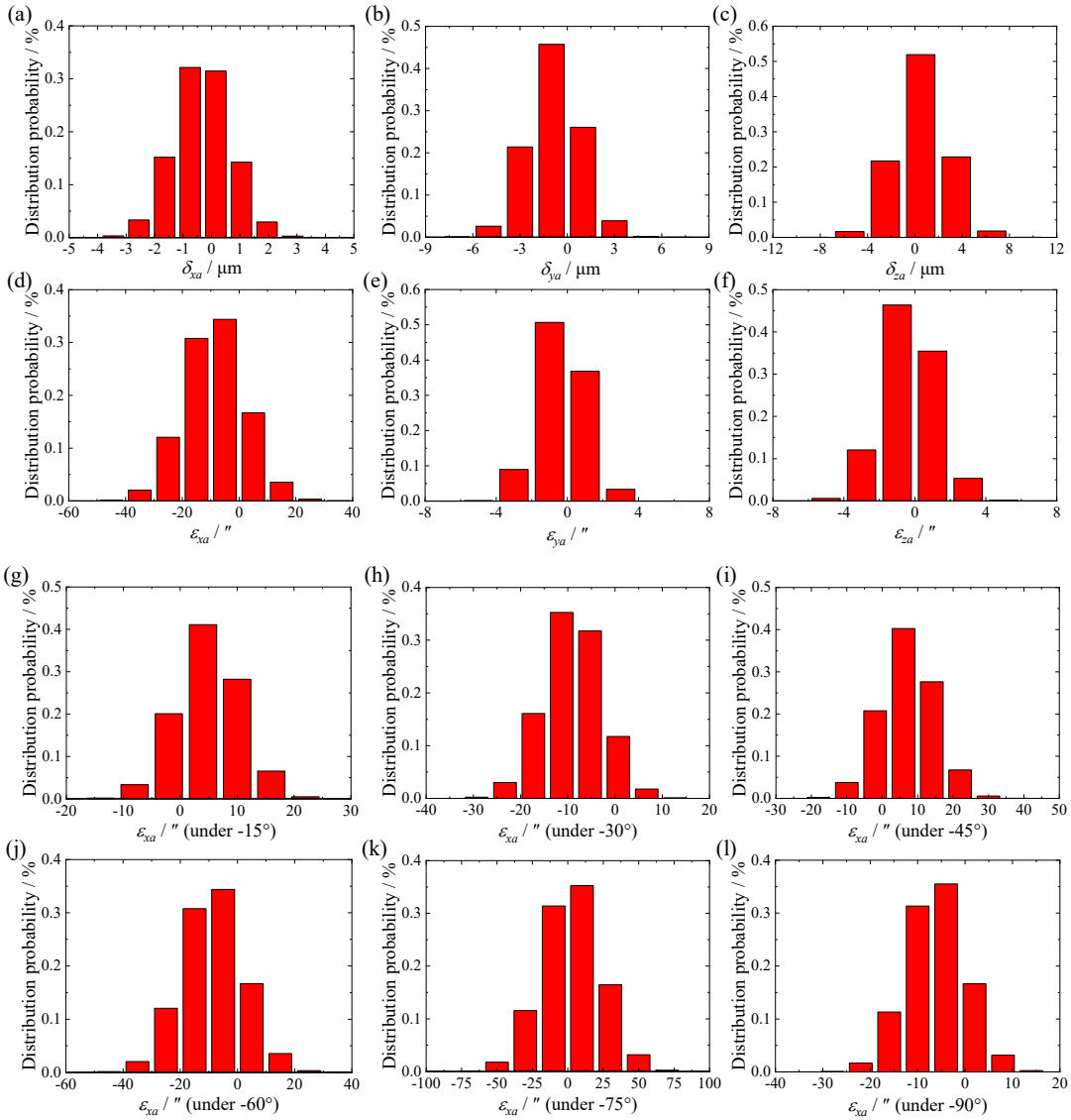

Figure 3. Identification results with the same rotation angle and ε_{xa} with different rotation angles.

Table 1. The mean value of the uncertainty evaluation for different angles of A-axis.

Error term	**Standard Uncertainty (μm)**	**Inclusion interval (μm)**	**Error term**	**Standard Uncertainty (″)**	**Inclusion interval (″)**
δ_{xa}	0.99	(δ - 1.94, δ + 1.94)	ε_{xa}	9.38	(ε - 18.40, ε + 18.40)
δ_{ya}	1.63	(δ - 3.21, δ + 3.20)	ε_{ya}	1.26	(ε - 2.48, ε + 2.48)
δ_{za}	2.13	(δ - 4.18, δ + 4.18)	ε_{za}	1.46	(ε - 2.86, ε + 2.86)

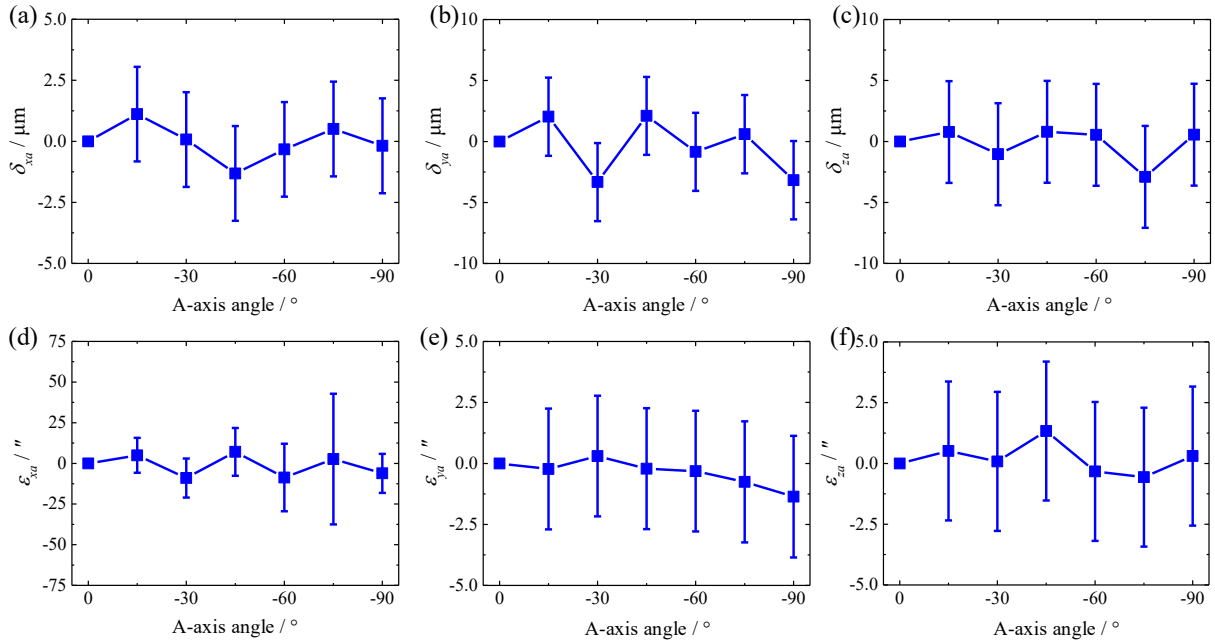

Figure 4. Identification results of A-axis PDGEs considering measurement uncertainty. Error bars represent the estimation uncertainty: (a) Position error δ_{xa}; (b) Position error δ_{ya}; (c) Position error δ_{za}; (d) Angle error ε_{xa}; (e) Angle error ε_{ya}; (f) Angle error ε_{za}.

4.2 Analysis of uncertainty evaluation results

When the sine and cosine term in the denominator tend to zero, it leads to large measurement uncertainty and result to large deviation from the true value. Therefore, for the A-axis, when a_n is close to -90°, the equation containing the sine term is used to identify ε_{xa}, which can effectively reduce the measurement uncertainty of the angular positioning error.

As shown in Figure 5, ε_{xa} of the A-axis under -60° and -75° is significantly reduced compared with that before optimization, and the uncertainty represented by the error bars tend to be stable under different angles.

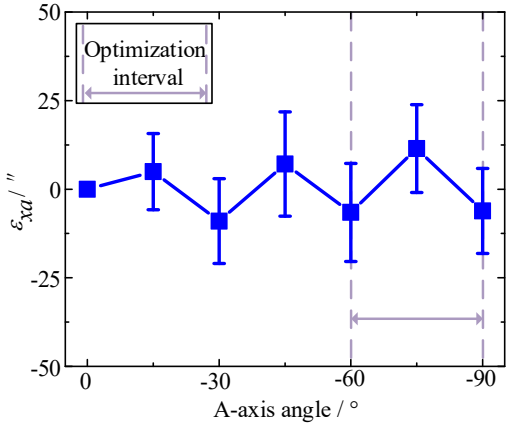

Figure 5. Identification results of the optimized angular positioning errors of A-axis.

The standard uncertainty of ε_{xa} is reduced from 9.38″ to 6.43″ and the inclusion interval is narrowed from (ε - 18.40, ε + 18.40) to (ε – 12.61, ε + 12.61), showing a decrease of about 30%.

5. CONCLUSIONS

(1) The rotary axis's PDGEs error model considering tool setting error, translational axis error and installation error is established. (2) The translational axis motion error and tool setting error are the main uncertainty sources in the PDGEs measurement uncertainty. (3) The PDGEs standard uncertainty of AC axis is stable, which verifies the validity of this study and can reflect the quality of the measurement results.

ACKNOWLEDGEMENTS

This research is sponsored by Key Research and Development Program of Ningbo (2021Z077).

REFERENCES

[1] Fu, G., Gong, H., Fu, J., Gao, H. and Deng, X., "Geometric error contribution modeling and sensitivity evaluating for each axis of five-axis machine tools based on POE theory and transforming differential changes between coordinate frames," International Journal of Machine Tools and Manufacture, 147, 103455(2019).

[2] Chen, Q., Li, W., Jiang, C., Zhou, Z. and Min, S., "Separation and compensation of geometric errors of rotary axis in 5-axis ultra-precision machine tool by empirical mode decomposition method," Journal of Manufacturing Processes, 68(A), 1509-1523 (2021).

[3] He, Z., Fu, J., Zhang, L. and Yao, X., "A new error measurement method to identify all six error parameters of a rotational axis of a machine tool," International Journal of Machine Tools and Manufacture, 88, 1-8(2015).

[4] Wang, J., Guo, J., Zhang, G., Guo, B. and Wang, H., "The technical method of geometric error measurement for multi-axis NC machine tool by laser tracker," Measurement Science and Technology, 23(4): 45003-45013(2012).

[5] Deng, M., Li, H., Xiang, S., Liu, P., Feng, X., Du, Z. and Yang, J., "Geometric errors identification considering rigid-body motion constraint for rotary axis of multi-axis machine tool using a tracking interferometer," International Journal of Machine Tools and Manufacture, 158, 103625(2020).

[6] Sepahi-Boroujeni, S., Mayer, J., Khameneifar, F. and Woźniak, A., "A full-covariance uncertainty assessment in on-machine probing," International Journal of Machine Tools and Manufacture, 167, 103768(2021).

[7] ISO/TR 230-9: Estimation of measurement uncertainty for machine tool tests according to series ISO 230, basic equations[S], (2005).

[8] ISO 14253-2: Inspection by measurement of workpieces and measuring equipment–Part 2: Guidance for the estimation of uncertainty in GPS measurement, in calibration of measuring equipment and in product verification[S], (2011).

[9] Zhou, T., Ye, D. and Sha, D., [Monte Carlo Method for Evaluation of Measurement Uncertainty: JJF1059.2—2012], Beijing: National Technical Committee of Legal Metrology Management, 5-11(2012).

[10] Liu, Y., Wan, M., Xiao, Q. and Zhang, W., "Identification and compensation of geometric errors of rotary axes in five-axis machine tools through constructing equivalent rotary axis (ERA)," International Journal of Mechanical Sciences, 152, 211-227(2019).

[11] Xiang, S. and Altintas, Y., "Modeling and compensation of volumetric errors for five-axis machine tools, International Journal of Machine Tools and Manufacture, 101, 65-78(2016).